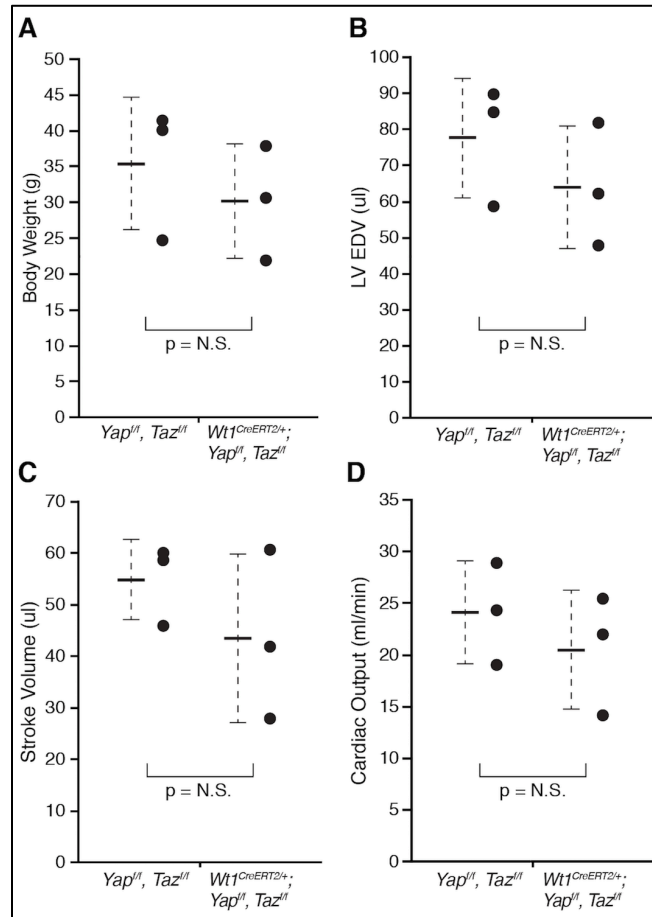
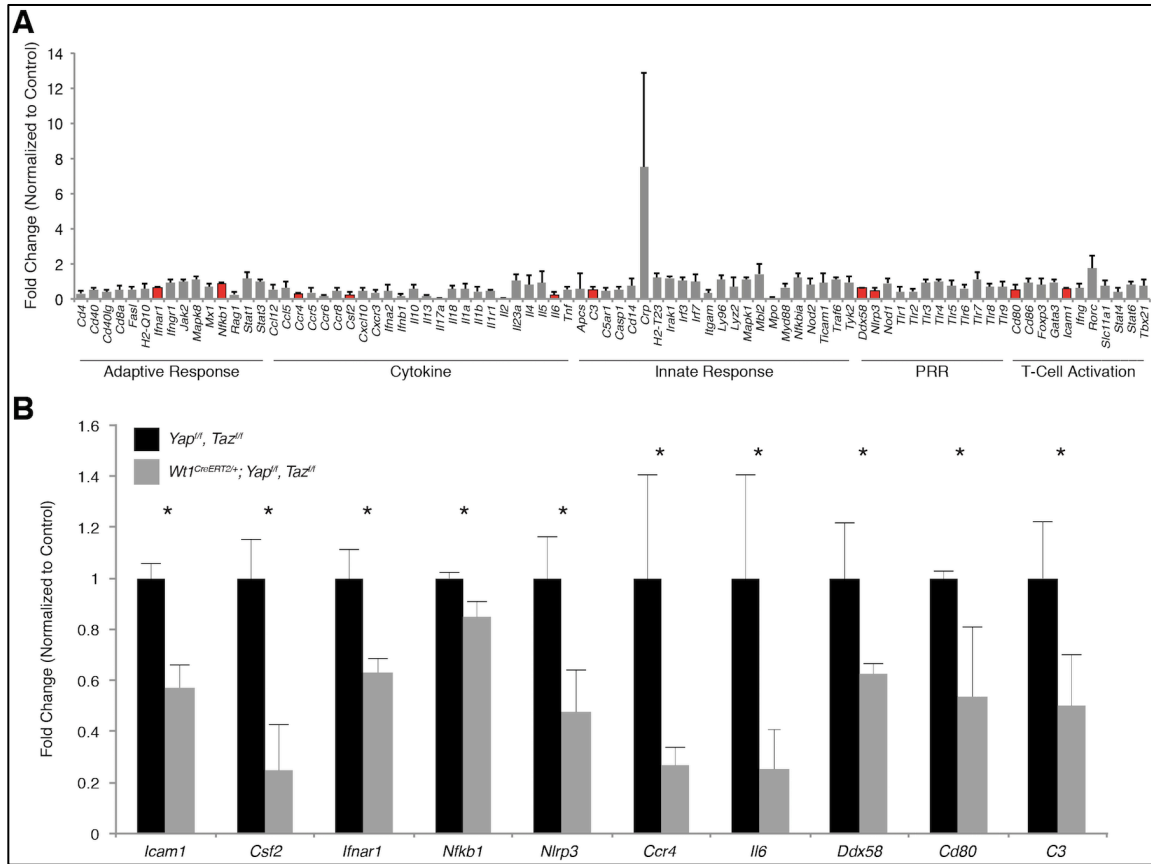


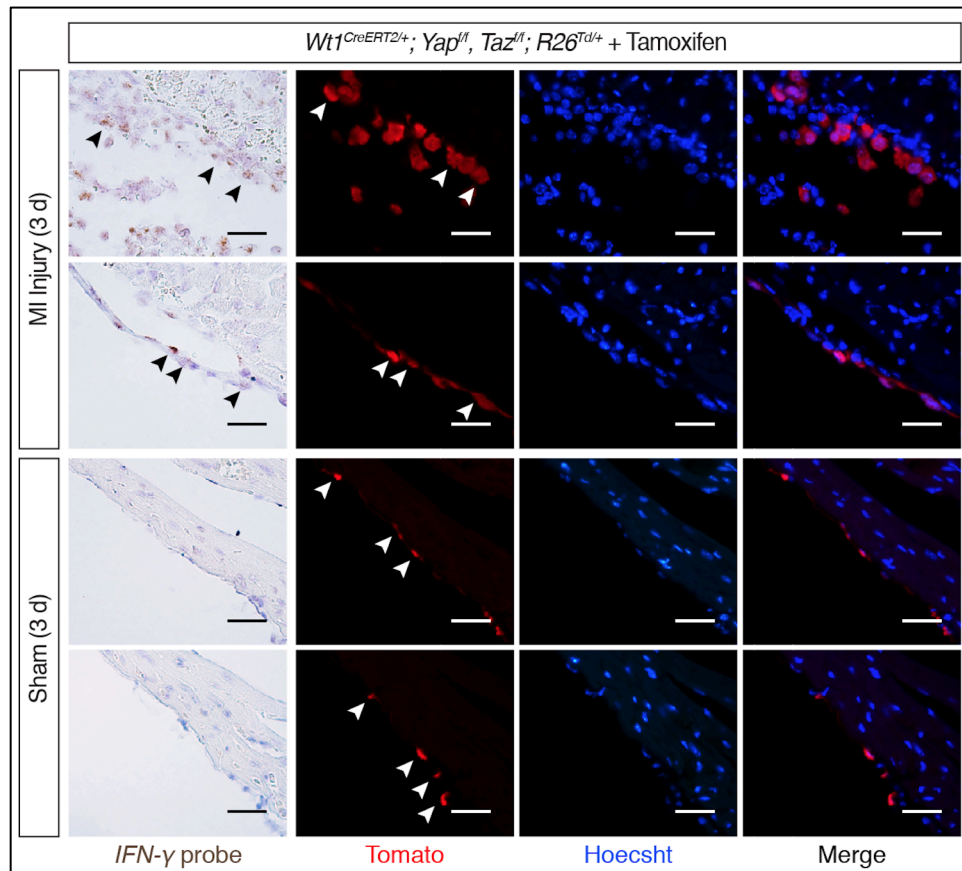
Supplemental Figure 1. Mutant and control mice demonstrate equal size injury region at 2 days post-LAD ligation. (A, B) Whole-mount images and histology of control (n=3) and mutant animals (n=4) as indicated, 2 days post-MI (LAD ligation). White dotted line demarcates area of injury near the ligature, and representative Trichrome staining of sections at base (i), mid-ventricle (ii), and apex (iii). (C) Quantification of fibrosis of serial sections; there is no statistical difference between fibrosis in mutant and control (P value was calculated using a two-tailed Student's t-test; Data represent mean \pm SEM) (D, E) Whole-mount images and histology of control (n=3) and mutant (n=3) 14 days after sham surgery. No excessive fibrosis is noted in the chest wall cavity or heart in the mutant (E). Representative histology images from base, mid-ventricle, and apex are shown in (D, E). (A-E) Tamoxifen administered to both control and mutant 2 days prior to and 2 days post surgery. Scale Bars: 1 mm.



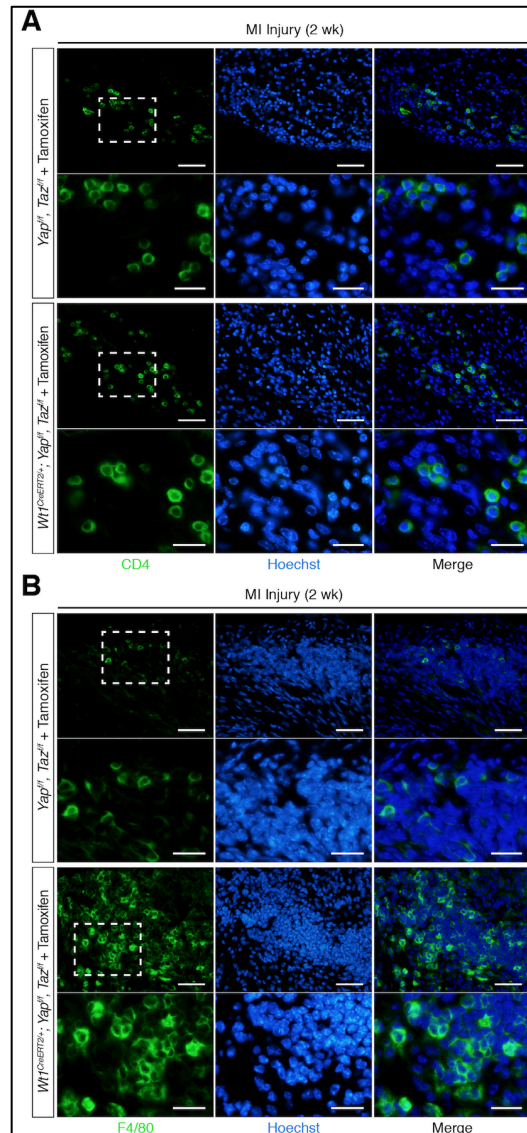
Supplemental Figure 2. Cardiac function in epicardial null mice and control mice are the same at baseline. Transthoracic echocardiography in 3 control ($Taz^{fl/fl}; Yap^{fl/fl}$) and 3 mutant mice ($Wt1^{CreERT2/+}; Yap^{fl/fl}; Taz^{fl/fl}$) after tamoxifen induction and no surgery at 1 week post-MI shows no significance difference in body weight (A), left ventricular end-diastolic volume (LV EDV) (B), stroke volume (C), and cardiac output (D). Data represent mean \pm SD. P values were calculated using a two-tailed Student's t-test. Significance: N.S. = not significant.



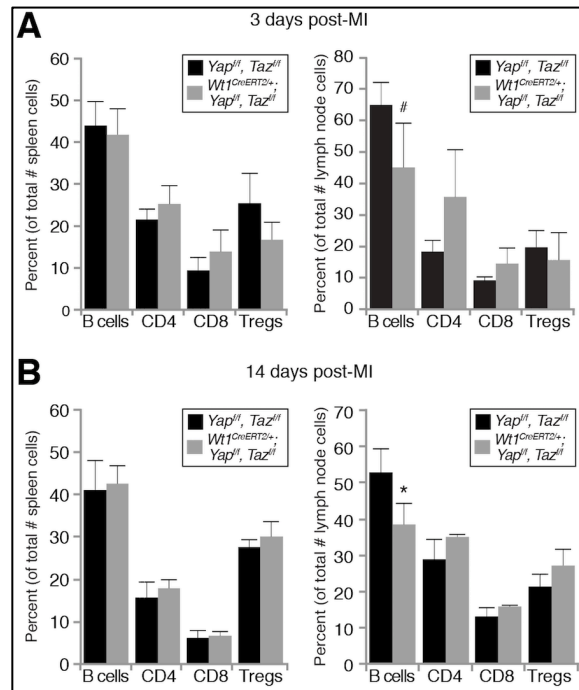
Supplemental Figure 3. Epicardial Yap/Taz null mice demonstrate alteration of multiple immune targets at 14 days post-MI. (A) Bar graph of quantitative RT-PCR immune arrays from microdissected free LV walls of control (*Yap^{fl/fl}; Taz^{fl/fl}*, n=3) and mutant (*Wt1^{CreERT2/+}; Yap^{fl/fl}; Taz^{fl/fl}*, n=3) animals at 14 days post-MI. Red targets represent significantly downregulated genes in mutants compared with controls (n=3 in both groups). (B) Bar graph showing specific fold changes for the 10 significantly modulated genes in the qRT-PCR immune arrays (n=3 in both groups). Statistics were completed using a Student's t-test. Data represent mean ± SD. Significance: *p < 0.05.



Supplemental Figure 4. *IFN-γ* is produced by epicardial activated cells after MI injury. Cross sections from *Wt1*^{CreERT2/+}; *Yap*^{flox/flox}; *Taz*^{flox/flox}; *R26*^{Tomato/+} animals following RNAscope *in situ* hybridization for *IFN-γ* 3 days after MI injury or sham surgery, as indicated (2 examples each). Black arrows denote *IFN-γ* positive cells in the epicardium, and white arrows denote corresponding tomato positive cells in the epicardium. Adjacent sections stained for Hoechst, Tomato or merged (Hoechst/Tomato) are shown as indicated. Scale bar: 25 μm.



Supplemental Figure 5. Epicardial Yap/Taz null mice exhibit a hyperinflammatory response. (A) Cross sections from *Yap^{fllox/fllox}; Taz^{fllox/fllox}* (control) and *Wt1^{CreERT2/+}; Yap^{fllox/fllox}; Taz^{fllox/fllox}* (mutant) animals 14 days post-MI immunostained for CD4 and/or Hoechst demonstrating a similar number of CD4+ T-cells in both groups. (B) Cross sections from *Yap^{fllox/fllox}; Taz^{fllox/fllox}* (control) and *Wt1^{CreERT2/+}; Yap^{fllox/fllox}; Taz^{fllox/fllox}* (mutant) animals 14 days post-MI immunostained for F4/80 and/or showing increased F4/80+ macrophages in the mutant mice compared to controls. Scale bars: 50 μ m (A, B; top panels for each genotype), 25 μ m (A, B; bottom panels for each genotype).



Supplemental Figure 6. Immune cell populations of the spleen and mediastinal lymph node are unchanged following epicardial Yap/Taz deletion. (A-B) Flow cytometry analyses of mediastinal lymph nodes and spleen 3 (A) and 14 (B) days post-MI from mutant ($Wt1^{CreERT2/+}; Yap^{flox/flox}; Taz^{flox/flox}$) and control ($Yap^{flox/flox}; Taz^{flox/flox}$) mice (n=3 in all analyses). Statistics were completed using a Student's t-test, Data represent mean \pm SD. Significance: [#]p < 0.10, and ^{*}p < 0.05.

Supplemental Table 1. Quantitative echocardiographic measurements demonstrate significantly reduced LV end-diastolic volume and chamber length in mutant mice after MI. Comprehensive echocardiographic measurements in *Taz^{fllox/fllox}*; *Yap^{fllox/fllox}* (control, n=7) and *Wt1^{CreERT2/+}*; *Yap^{fllox/fllox}*; *Taz^{fllox/fllox}* (mutant, n=6) animals one week post-MI show significantly reduced LV end-diastolic volume, LV diastolic endocardial length and LV systolic endocardial length in epicardial Yap/Taz null mice. Means and standard deviations are shown for each corresponding metric. P values were calculated using a two-tailed Student's t-test.

	LVAEpid	LVAENDd	LVAEN Ds	LVLd	LVLs	EDV	ESV	SV	CO	HR	LVmass	LVmass/BW	IVSd	IVSs	LVPWd	LVPWs	LVDd	LVDs
	mm ²	mm ²	mm ²	mm	mm	ul	ul	ul	ml/min		mg	mg/g	mm	mm	mm	mm	mm	mm
CONTROLS (N=7)																		
Mean	29.037	14.970	8.832	8.269	7.707	103.533	57.254	46.279	21.863	472	126.005	4.134	0.905	1.239	0.752	1.017	4.116	3.073
Std deviation	4.408	1.160	1.678	0.781	0.890	15.679	15.208	3.882	2.359	25	43.850	1.084	0.229	0.302	0.149	0.195	0.302	0.386
MUTANTS (N=6)																		
Mean	25.381	13.960	8.073	7.297	6.792	85.262	46.714	38.548	15.889	409	90.074	3.849	0.829	1.156	0.748	1.057	3.972	2.874
Std deviation	6.569	2.797	2.910	0.554	0.694	19.930	20.576	7.710	4.787	86	38.104	0.961	0.192	0.198	0.217	0.196	0.260	0.421
P value	0.257	0.399	0.569	0.027	0.066	0.091	0.311	0.039	0.014	0.091	0.146	0.629	0.535	0.578	0.966	0.723	0.381	0.392

LEGEND

BW	grams	Body weight
HR	bpm	Heart rate
LVAEpid	mm ²	LV epicardial area at end diastole
LVAENDd	mm ²	LV endocardial area at end diastole
LVAENDs	mm ²	LV endocardial area at end systole
LVLd	mm	LV length from plane of the mitral valve to the apical endocardial surface during diastole
LVLs	mm	LV length from plane of the mitral valve to the apical endocardial surface during systole
EDV	ul	End diastolic LV volume
ESV	ul	End systolic LV volume
SV	ul	Stroke volume
CO	ml/min	Cardiac output
HR		Heart rate
IVSd	mm	Thickness of the Interventricular septum in diastole
IVSs	mm	Thickness of the Interventricular septum in systole
LVPWd	mm	LV posterior wall thickness, diastole
LVPWs	mm	LV posterior wall thickness, systole
LVDd	mm	LV dimension in diastole
LVDs	mm	LV dimension in systole